JOURNAL OF CATALYSIS 36, 30-35 (1975)

Studies on Pore Structure of Adsorbents and Catalysts

II. Pore Size Distribution in Synthetic Chrysotile: The Classical and Corrected Kelvin Equation Applied to Nitrogen Capillary Condensation

L. A. DE WIT AND J. J. F. SCHOLTEN*

Department of Chemical Technology, Delft University of Technology, Julianalaan 136, Delft-2208, The Netherlands

Received February 1, 1974

The pore size distribution in two samples of synthetic chrysotile has been determined from nitrogen capillary condensation. Comparison of the results with the distribution found from electron microscopy (see Part I) leads to the conclusion that in the range of pore radii from 20 to 70 Å the Kelvin equation, corrected according to Broekhoff and de Boer, is confirmed much better than the classical Kelvin equation. This finding has important consequences for the practice of texture studies on heterogeneous catalysts and other porous substances, since the corrections involved in the range of radii indicated amount to 20–30%.

INTRODUCTION

In a series of articles published in this journal, Broekhoff and de Boer (*1–6*) have shown that it is necessary, on theoretical grounds, to introduce corrections into the classical Kelvin equation, especially when this is applied to very small pores, cavities, and slits, as in the calculation of pore size distributions in catalysts and other porous substances. A full account can be found in the thesis of Broekhoff (*7*), and a shorter treatment by Broekhoff, which also presents the fundamental numerical relationships needed for applying the theory, is also available (*8*).

One of the essential points in the work of Broekhoff and de Boer is that in the derivation of the Kelvin equation describing nitrogen capillary condensation in very small pores, the thermodynamic potential of the liquid nitrogen in the pore is to be corrected by a term accounting for the influence of van der Waals adsorption forces emanating from the pore walls:

$$\mu_a(t) = \mu_L{}^0 - F(t). \qquad (1)$$

where $\mu_a(t)$ is the thermodynamic potential of nitrogen exposed to the action of adsorption forces, $\mu_L{}^0$ is the thermodynamic potential of liquid nitrogen *per se*, and $F(t)$ is a function which can be determined from the so-called t-curve (*9*) describing multimolecular adsorption on a flat surface of the material under investigation; t denotes the thickness of the adsorbed layer.

The corrections arising from the Broekhoff–de Boer theory start by assuming significant proportions at pore radii of 5000 Å and below. By way of example a comparison is made in Table 1 between the radii of cylindrical pores calculated from the classical Kelvin equation, and those found from the corrected equation.

Table 1 shows that considerable corrections are involved, especially below r = 1000 Å. Hence, if the Broekhoff–de Boer theory is correct, it has important consequences for all work in which pore size distributions are calculated by means of the Barrett–Joyner–Halenda method (*10*) in

---

* To whom all correspondence should be directed.

TABLE 1

RADII OF CYLINDRICAL PORES CALCULATED FROM THE CLASSICAL KELVIN EQUATION AND COMPARED WITH THE RADII FOLLOWING FROM THE KELVIN EQUATION CORRECTED ACCORDING TO BROEKHOFF AND DE BOER

Classical Kelvin equation—pore radius (Å)	Corrected equation—pore radius (Å)	Correction (%)
4097.0	4280.0	4.5
843.0	927.6	10.0
472.3	535.0	13.3
327.8	380.2	16.0
251.3	295.5	17.6
83.9	101.8	21.4
47.6	58.3	22.6
30.8	38.3	24.3
23.3	29.5	26.3
15.3	19.9	30.3

combination with the *classical* Kelvin equation. Hence, a search has to be made for direct experimental confirmation of Broekhoff and de Boer's theory; this can be done by measuring the capillary condensation of nitrogen in materials containing small pores of known dimensions.

In the first paper of this series (*11*) we described the preparation, structure, and morphology of synthetic chrysotile, $Mg_3(OH)_4 \cdot Si_2O_5$, which consists of hollow needles of perfect cylindrical shape. The internal radii of these needles lie in the range from 20 to 70 Å, with a maximum around 40 Å, so this material is very well suited for our purpose. This article presents the nitrogen adsorption and desorption isotherms measured on synthetic chrysotile. The pore size distribution has been calculated from both the adsorption and desorption branches of the isotherms, with application of the corrected and classical Kelvin equations, and the results have been compared with the pore size distribution found from electron microscopy (*11*).

EXPERIMENTAL

All measurements were performed by means of a micro BET apparatus as described by Lippens *et al.* (*12*). A sample of synthetic chrysotile, (sample B, the synthesis and properties of which are described in Part I (*11*)) was used as the starting material. One part, sample B 1, was placed in the adsorption apparatus in the form of a loosely packed powder, whereas sample B 2 was studied in the form of highly compressed granules (pressure 3500 kg/cm^2). Before measuring the nitrogen adsorption isotherms at −196°C, the system was evacuated for 16 hr, the sample temperature being 120°C.

RESULTS

Figure 1 shows the nitrogen adsorption isotherm at −196°C as measured on sample B 2, the amount of physically adsorbed nitrogen being plotted as a function of the

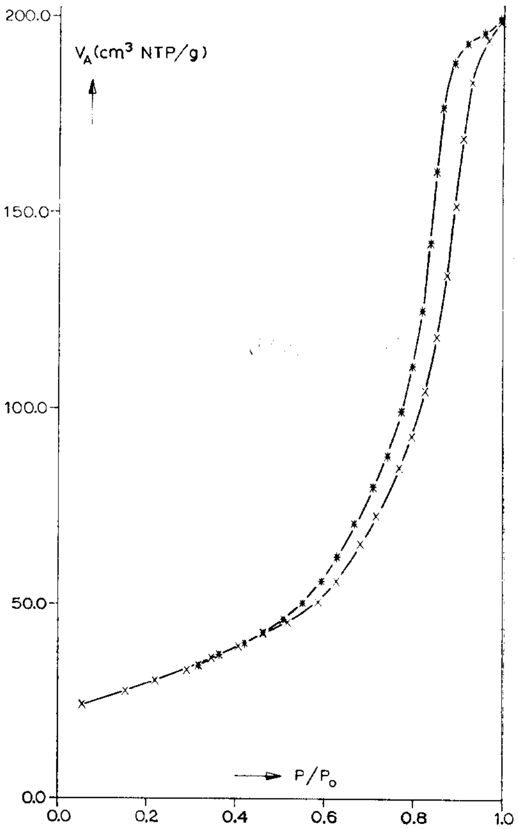

FIG. 1. Physical adsorption isotherm of nitrogen on chrysotile, sample B 2, at −196°C. The amount of nitrogen adsorbed (in cm^3 gas NTP/g) is plotted as a function of the relative nitrogen pressure.

relative pressure. Taking the cross-sectional area of a nitrogen molecule as 16.2 Å^2, the BET surface area calculated from this isotherm equals 103.4 m^2/g, in quite good accordance with the area found from electron microscopy (*11*), viz. 93 m^2/g.

The total pore volume is composed of a large amount of intercrystalline cavities of irregular shape (the needles will only partly be stacked parallel), and a smaller pore volume, formed by the perfectly cylindrical pores (open at both ends) *inside* the needles. Nevertheless, the shape of the hysteresis loop is A-type, according to the classification of de Boer (*13*), which would point to the presence of cylindrical pores only. This again demonstrates, as pointed out earlier by Broekhoff (*6*), that the predictive value of the shape of the hysteresis loop is very limited.

For sample B 2 a complete pore size analysis was performed on the basis of both the adsorption and the desorption branches of the isotherm. Use was made of a computer program developed with the aid of the calculation scheme of Barrett, Joyner, and Halenda (*10*), and of the *classical* Kelvin equation for cylindrical pores open at both ends. The result is shown in Fig. 2, where $d(V/M)/dr$, the derivative of the pore volume per unit weight with respect to the pore radius, is plotted as a function of the pore radius.

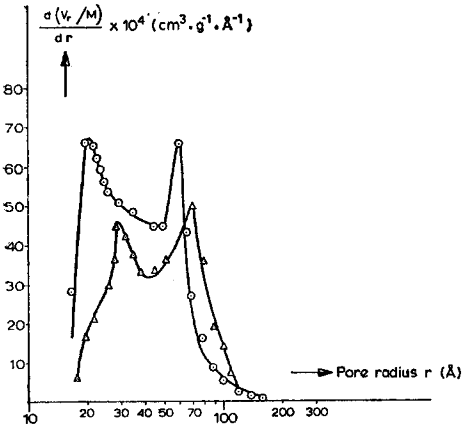

FIG. 2. Pore size distribution in compressed granules of chrysotile, sample B 2. The analysis is made by means of the classical Kelvin equation. The derivative of the pore volume per unit mass is plotted as a function of the pore radius (log scale). ⊙, calculated from the adsorption isotherm; △, calculated from the desorption isotherm.

The following points are striking:

> The pore size distribution analysis relating to the adsorption branch is not consistent with that relating to the desorption branch. This is a well-known shortcoming of this method of analysis.
>
> The distribution is bimodal, obviously owing to the fact that we are confronted here with the internal pore size distribution of the circular pores open at both ends *inside* the chrysotile needles and the external pore size distribution of the intercrystalline cavities *between* the chrysotile needles.
>
> The maxima in the internal pore size distribution are located at a pore radius of 20 and 30 Å, respectively. Both values are significantly lower than the maximum found from electron microscopy (40 Å), the deviation being greatest for the distribution relating to the *ad*sorption branch of the isotherm.
>
> The maxima in the external pore size distribution peaks lie at 62 and 70 Å, respectively; in this range of pore sizes the distributions found from the two branches are more near to each other.

Next, we analyzed the nitrogen isotherm of sample B 2, but now with the aid of the Barrett–Joyner–Halenda method incorporating the *corrected* Kelvin equation. The result is plotted in Fig. 3.

It is immediately seen that the distributions found from the adsorption and desorption branches of the isotherm are now consistent throughout the range of pore radii measured. Another, and more important point, is that the maxima in the internal pore size distribution now lie at 34 Å (adsorption branch) and 38.5 Å (desorption branch), respectively. These values are much closer to that found from electron microscopy, i.e., 40 Å.

It is of course possible that the internal pore size distribution, represented by the

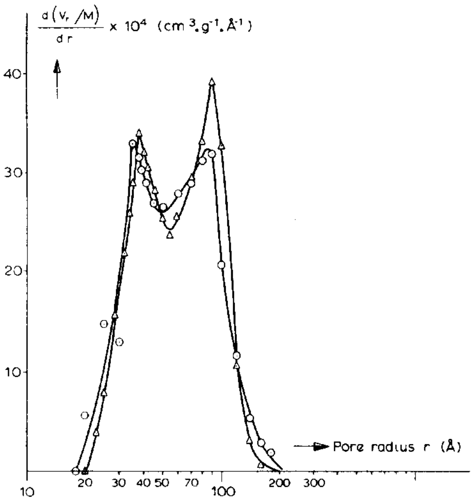

FIG. 3. Pore size distribution in compressed granules of chrysotile, sample B 2. The analysis is made by means of the *corrected* Kelvin equation. The derivative of the pore volume per unit mass is plotted as a function of the pore radius (log scale). ⊙, calculated from the adsorption isotherm; △, calculated from the desorption isotherm.

left peak in Fig. 3, is not exclusively caused by the pores *inside* the chrysotile needles, but also reflects some contribution from intercrystalline pores, formed, for instance, by the cavities between three or more closely packed equally oriented chrysotile needles. Such cavities, though not cylindrical in shape, come in the same size range as the pores *within* the needles. Evidence for this is found in the pore size analysis of the loosely packed sample B 1 (Fig. 4). It is seen here that, owing to the larger distance between the needles, the internal and external distribution peaks are much further apart. As found in the compacted sample B 2, the maximum in the internal pore size distribution of the chrysotile needles is situated at 38.5 Å (desorption branch); further the integrated volume of the left-hand peak is smaller than that for the compacted sample while the maximum lies at a lower value of $d(V/M)/dr$.

The distribution peak of the intercrystalline cavities is a maximum at $r = 145$ Å, the corresponding figure for the compact sample B 2 being 70 Å. This shift, too, points to a greater sparsity of the needles.

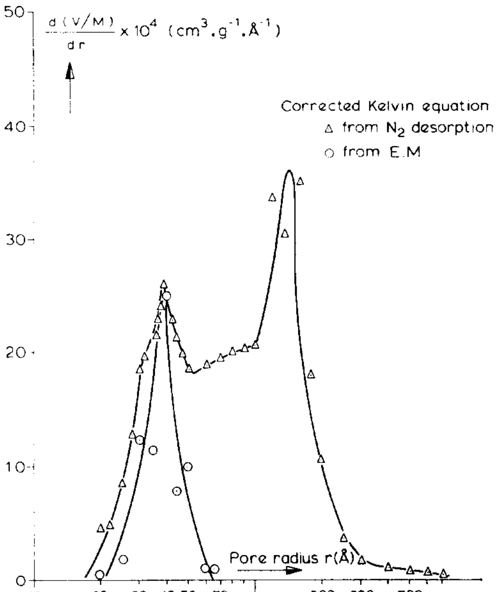

FIG. 4. Pore size distribution in loosely packed chrysotile powder, sample B 1. The analysis is made by means of the *corrected* Kelvin equation. The derivative of the pore volume per unit mass is plotted as a function of the pore radius (log scale). Open triangles, calculated from the desorption branch of the nitrogen isotherm; open circles, pore size distribution found from electron microscopy.

Finally, in Fig. 4 we have plotted the internal pore size distribution in synthetic chrysotile as determined by electron microscopy. This distribution was taken from Fig. 4 in Part I (*11*), and relates to the same preparation B as discussed here. It is seen that the pore size distribution calculated by means of the Kelvin equation corrected according to Broekhoff and de Boer, is confirmed rather well by direct electron microscopic observation.

DISCUSSION

We may state that the corrected Kelvin equation yields reliable results in those cases where the pores are really cylindrical. As seen from the experimental angle, it is desirable to extend the measurements, using a chrysotile sample in which the crystallites are *totally* separate; work in this direction is in progress. Furthermore, experiments with preparations containing circular pores of larger radii than those in synthetic chrysotile have to be performed. From the literature it appears that some natural chrysotile samples contain pores somewhat wider than those in the synthetic product, and perhaps these will be suitable for our purpose.

As we see it, there are now sufficient reasons for replacing the classical Kelvin equation by the corrected one in all computer programs used in the determination of pore size distributions, because the corrections involved are fairly large (see Table 1) and well established experimentally for pores with radii in the range of 40 Å.

On the other hand, further refinements in the Broekhoff–de Boer theory are perhaps still possible, especially in the range of pores with radii lower than, say, 40 Å. As stated by Broekhoff (*8*), a number of estimations and suppositions underlie the theory. For instance, it is supposed that thermodynamic methods may be applied notwithstanding the fact that the number of nitrogen molecules which can be spread out over the length of the pore radius is only of the order of ten, for instance in the case of 20 Å pores. Furthermore, it is supposed that the density of the adsorbed nitrogen and its surface tension do not differ significantly from those of free liquid nitrogen at the same temperature. (The same suppositions hold, of course, in the classical Kelvin theory.)

As to the surface tension, recent statistical thermodynamic calculations by Woon Sun Ahn *et al.* (*14*) have shown that the surface tension of a concave liquid nitrogen surface in fact increases with decreasing radius of curvature. Theoretically, the surface tension of liquid nitrogen at 77.34 K should be of the order of 10% higher for a concave nitrogen surface with a radius of curvature of 55 Å, than that of the flat surface, and at a radius of curvature of 20 Å it should be even 40–50% higher.

As can be seen in Fig. 4, the discrepancy between the results from nitrogen capillary condensation and from electron microscopy in the range of pores with radii of about 20 Å is of the order of 30%. Introduction of the surface tensions of concave liquid nitrogen surfaces, as given by Woon Sun Ahn *et al.* in the corrected Kelvin equation would lead to a somewhat better agreement. The corrected Kelvin equation which holds for adsorption and capillary condensation in cylindrical pores open at both ends, reads:

$$RT \ln(p/p_0) - F(t) = \gamma \cdot V_L/(r - t), \quad (2)$$

where R is the gas constant, T the absolute temperature, p/p_0 the relative nitrogen pressure, $F(t)$ the correction discussed in the Introduction, γ the surface tension of nitrogen, V_L the molar volume of the liquid phase, r the pore radius and t the thickness of the adsorbed layer. One sees from Eq. (2) than an increase in the surface tension of 40–50% leads to a percentage correction of the same order in the pores radius r.

Another supposition in the Broekhoff–de Boer theory is that the so-called "common *t*-curve" is applicable to the surface under investigation (*8*). The common *t*-curve applies to flat oxide surfaces, but we have found that it does hold for chrysotile, notwithstanding the surface being strongly bent. The fact that 80% of the surface area is formed by the less strongly bent external surface of the needles makes the result comprehensible.

In the third article of this series the results of mercury penetration into chrysotile will be compared with those of electron microscopy and nitrogen capillary condensation. A preliminary short communication of this work has been published (*15*).

ACKNOWLEDGMENTS

Thanks are due to Dr. J. C. P. Broekhoff and Dr. J. C. Rasser for helpful discussions. Dr. Broekhoff provided us with a computer program including the classical Kelvin equation (Fig. 2). A large part of the experimental work was carried out by Mr. J. A. Konvalinka and by Mr. J. Teunisse.

REFERENCES

1. BROEKHOFF, J. C. P., AND DE BOER, J. H., *J. Catal.* **9**, 8 (1967).

2. BROEKHOFF, J. C. P., AND DE BOER, J. H., *J. Catal.* **9**, 15 (1967).

3. Broekhoff, J. C. P., and de Boer, J. H., *J. Catal.* **10,** 153 (1968).
4. Broekhoff, J. C. P., and de Boer, J. H., *J. Catal.* **10,** 368 (1968).
5. Broekhoff, J. C. P., and de Boer, J. H., *J. Catal.* **10,** 377 (1968).
6. Broekhoff, J. C. P., and de Boer, J. H., *J. Catal.* **10,** 391 (1968).
7. Broekhoff, J. C. P., "Adsorption and Capillarity," Thesis for Delft University of Technology, Waltman, Delft, 1969.
8. "Physical and Chemical Aspects of Adsorbents and Catalysts" (B. G. Linsen, Ed.), Chapter I, pp. 1–59. Academic Press, London and New York 1970.
9. de Boer, J. H., Lippens, B. C., Linsen, B. G., and Osinga, Th. J., *J. Colloïd Interface Sci.* **21,** 405 (1966).
10. Barrett, E. P., Joyner, L. G., and Halenda, P. P., *J. Amer. Chem. Soc.* **73,** 373 (1951).
11. Scholten, J. J. F., Beers, A. M., and Kiel, A. M., *J. Catal.* **36,** 23 (1974).
12. Lippens, B. C., Linsen, B. G., and de Boer, J. H., *J. Catal.* **3,** 32 (1964).
13. de Boer, J. H., *in* "The Structure and Properties of Porous Materials" (D. H. Everett and F. S. Stone, Eds.), p. 68. Butterworth, London, 1958.
14. Woon Sun Ahn, Mu Shik Jhon, Hyungsuk Pak, and Seihun Chang, *J. Colloïd Interface Sci.* **38,** 605 (1972).
15. de Wit, L. A., Beers, A. M., and Scholten, J. J. F., *Delft Progr. Rep.* **1,** 29 (1973).